Eur. Phys. J. E (2011) **34**: 6
DOI 10.1140/epje/i2011-11006-y

THE EUROPEAN PHYSICAL JOURNAL E

Regular Article

Surface nucleation in the crystallisation of polyethylene droplets

J.L. Carvalho and K. Dalnoki-Veress[a]

Department of Physics & Astronomy and the Brockhouse Institute for Materials Research, McMaster University, Hamilton, ON, Canada

Received 22 September 2010
Published online: 12 January 2011 –

Abstract. The division of semi-crystalline polymeric material into small domains is an effective tool for studying crystal nucleation. The scaling behavior of the nucleation rate as a function of domain size can reveal important information about the mechanism responsible for the birth of a crystal nucleus. We have investigated the process of crystal nucleation in a system of dewetted polyethylene droplets. Through the use of a correlation sample analysis, we are able to differentiate between heterogeneous and homogeneous nucleation mechanisms in a droplet sample. An analysis of the dependence of the nucleation rate on droplet size reveals that the nucleation probability scales with the surface area of the droplet.

1 Introduction

Inspired by the classic nucleation experiments of Vonnegut [1] and Turnbull [2] on finely dispersed metallic domains, systems of polymer droplets have long proven to be successful for studies on polymer crystal nucleation. Such systems overcome the difficulty of studying nucleation in the bulk, where growth kinetics convolutes measurements of the nucleation rate. The simple concept behind these types of experiments is illustrated in fig. 1, and can be understood as follows. A crystallizable material will contain heterogeneities, defects from which a crystal nucleates. These heterogeneities lower the activation barrier to nucleation and hence bulk systems are typically dominated by *heterogeneous* nucleation. In contrast, *homogeneous* nucleation is an intrinsic material property and represents the true activation barrier to nucleation. In fig. 1a), a schematic sample contains four defects and is divided up into four domains. Thus, each domain is dominated by heterogeneous nucleation. However, by subdividing the material into smaller domains, as shown in fig. 1b), such that the number of domains exceeds the number of defects or heterogeneities, true homogeneous nucleation may be observed. Simply put, by subdividing the bulk sample into many small, isolated domains, each domain can act as a separate nucleation experiment. These systems can provide the necessary statistics to properly access information on the nucleation process. Researchers have achieved such samples through a number of geometries, including polymer droplets dispersed in immiscible matrices [3–7], droplets sprayed on slides [8], phase-separated block copolymers [9–14], alumina nanopores [15], and dewetted polymer droplets [16–21]. We have shown previously that

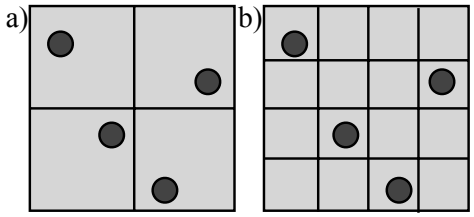

Fig. 1. Schematic of the principle behind subdividing a crystallizable material into small domains. The circles represent heterogeneities. a) Material divided into four domains, each containing a heterogeneity. b) Material subdivided into 16 compartments of which four crystallize heterogeneously, and the remaining domains can only crystallize via homogeneous nucleation.

with dewetted droplets large populations of domains are defect-free, facilitating an understanding of the differences between the *defect-driven* heterogeneous and *intrinsic* homogeneous nucleation mechanisms [16,17,19], melt memory of previous nuclei [18], and distinguishing between bulk, surface, and edge nucleation [21].

Crystalline polymers which have been subdivided into small micro-domains commonly exhibit what has been termed crystal fractionation upon cooling below the melting temperature [5]. This can be attributed to the fact that heterogeneities of varying nucleating ability are present. Less active heterogeneities —those that do not reduce the activation barrier significantly— will require greater supercooling to nucleate a crystal within a domain, than heterogeneities that have a high nucleating ability. As a result, a wide range of crystallisation temperatures is seen, corresponding to the different populations of heterogeneities. Only when the number of micro-domains

[a] e-mail: dalnoki@mcmaster.ca

exceeds the number of heterogeneities in the system does homogeneous nucleation in the defect-free domains become possible. When this is the case, the lowest temperature where nucleation takes place corresponds to the population of homogeneously nucleated droplets. Clearly, as the size of the micro-domains is made smaller, the population of homogeneously nucleated domains can increase significantly as more droplets are likely to be defect-free.

In experiments where fractionated nucleation was observed, the population of droplets displaying the lowest crystallisation temperature is often attributed to homogeneous nucleation based solely on this observation. Barham and coworkers, however, have cautioned that the observation of the lowest temperature may not be enough evidence for a homogeneous mechanism [8]. In a study of small polyethylene (PE) droplets prepared on glass slides, these researchers noted that the reproducibility of results was strongly dependent on the preparation of the slide. In particular, by using a number of different materials to coat the surface of the slide, they were able to produce a widely varying range of crystallisation temperatures. Some of the substrates resulted in nucleation temperatures even lower than those that previous researchers attributed to homogeneous crystallisation in similar PE droplet systems. Barham and coworkers suggested that the interface was playing an important role and that in fact *surface nucleation* may have been observed in previous studies. More recently, Lorenzo and co-workers investigated crystallisation within a sphere-forming diblock system [11]. They measured a lower nucleation temperature for the crystallizable PE spheres than that of Loo and co-workers [9] for similar PE domains. The crucial difference between the two studies was the interface of the confining medium: a hard glassy or soft melt matrix. As in the study by Barham *et al.*, Lorenzo *et al.* speculated that the specific nature of the interphase was playing an important role in nuclei formation and that conclusions about the nature of the nucleating mechanism could not easily be drawn.

In this study, we investigate nucleation within a system of dewetted PE droplets. We have previously demonstrated the use of the dewetting technique for studying nucleation in poly(ethylene oxide) (PEO) [16,17,19,21] and hydrogenated polybutadiene [18]. The dewetting process naturally produces small, isolated droplets over a range of length scales. A combination of the fast growth kinetics at the temperatures investigated combined with the small size of the domains means that once a crystal is nucleated within a droplet, the remaining material crystallises instantaneously on the timescale of the experiment. This separation of timescales makes the ability to study nucleation separate from crystal growth possible in dewetted polymer droplets. PE remains to be one of the most studied crystalline polymer systems, in part due to its simple structure, making it an ideal model system. However, despite its widespread use, questions remain as to the nature of the nucleating mechanisms. Through the use of correlation plots, which will be described in detail later, we are able to differentiate between homogeneous and heterogeneous nucleation in dewetted droplets of PE. Furthermore, for the homogeneous population of droplets, we investigate the nucleation rate as a function of droplet size. In our previous work, we have been able to conclusively demonstrate a volume-dependent nucleation rate for droplets of PEO using this technique [17,19]. Such direct evidence is lacking for PE. Here we show for the first time that homogeneous nucleation is *surface-induced* for PE droplets on a PS substrate. These results are in agreement with the suggestions of previous researchers as to the importance of the interface in PE droplet systems [8,11].

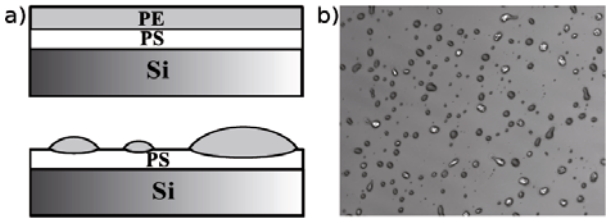

Fig. 2. (a) Schematic diagram of the initial sample geometry (top). Upon annealing above the melting temperature of PE, the PE film breaks up into isolated micron-sized droplets on a PS substrate (bottom). (b) Optical microscopy image of PE droplets (width 500 μm). When a PE droplet crystallises, it appears bright.

2 Experiment

The polymer used in these experiments are high molecular weight polystyrene (PS) ($M_w = 1246\,\mathrm{kg/mol}$, with polydispersity index $M_w/M_n = 1.06$, Polymer Source Inc., Canada) and linear PE ($M_w = 32.1\,\mathrm{kg/mol}$, $M_w/M_n = 1.1$, NIST Standard Reference Material 1483). Thick PS films ($h \sim 120\,\mathrm{nm}$) were spincast from toluene solutions onto clean Si substrates. The films were annealed at 160 °C for at least 5 hours under vacuum to remove residual solvent and relax the polymer chains. PE films ($h \sim 40$ to 90 nm) were spincast from hot 1,2-dichlorobenzene solution, using a filter to reduce heterogeneities (Millipore, 0.2 μm high temperature filters), onto freshly cleaved mica. A PE film was then floated onto a water surface (Milli-Q), and picked up off the water with the PS-Si substrate. The result was a layered film of PE-PS-Si. Upon annealing the sample at 160 °C for 36 hours under vacuum, the PE film dewetted from the unfavourable PS surface. This resulted in a system of small isolated PE droplets on a smooth PS substrate (fig. 2). The annealing temperature of 160 °C is above the glass transition temperature for PS ($T_g \sim 98\,^\circ\mathrm{C}$). This was necessary as the annealing temperature had to be above the melting temperature for PE ($T_m \sim 144\,^\circ\mathrm{C}$) [22] in order for the PE film to dewet. However, given the high molecular weight of the PS film combined with the unfavourable surface interaction between the two polymer species, the interface between PS and PE remains sharp and is depressed by the presence of the droplet as shown schematically in fig. 2a). We note that in dewetted droplets, because the contact angles are given by the interfacial tensions and independent of droplet size, all droplets are self-similar and the base

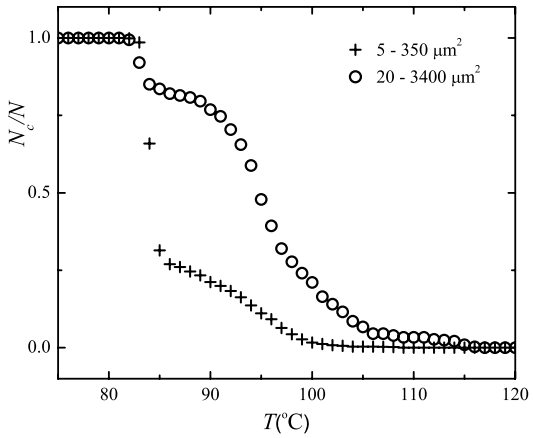

Fig. 3. The fraction of crystallized droplets for two samples with different droplet size distributions upon cooling from the melt at 1 °C/min. Size ranges listed correspond to the droplet base areas as measured by optical microscopy. For the larger droplet sample, the majority of droplets crystallize over a broad temperature range characteristic of heterogeneous nucleation. For the smaller droplet sample, the majority of droplets crystallize around the lowest temperature, $T_c \sim 84\,^{\circ}\mathrm{C}$.

area of a droplet, $A^{3/2} \propto$ volume. Following vacuum annealing, samples were transferred to an optical microscope heating stage (Linkam, UK) flushed with nitrogen gas for the crystallisation experiments. Samples were annealed on the heating stage at 160 °C for 40 min prior to crystallisation to erase thermal history. Crystallisation was followed with optical microscopy by nearly crossed polarizers and both the time at which a droplet nucleates and the base area of the droplet was obtained. Under these conditions, amorphous PE droplets appear dark, whereas crystallised droplets appear bright (fig. 2b)). The droplet base area and crystallisation time was tracked for each individual droplet. The length scale data could then be correlated to the crystallisation time, and the homogeneous population identified separately from the heterogeneous population, based on the crystallisation temperature.

3 Results and discussion

3.1 Crystallization upon cooling

As is commonly seen in dispersed systems, fractionated crystallisation was observed for the dewetted PE droplets upon cooling from the melt at 1 °C/min. To illustrate this effect, two droplet samples of differing size distributions were prepared by changing the thickness of the initial PE film. When a thicker film is used, the distribution of droplet sizes after dewetting is larger than for a thinner initial PE film. A sample with a large range in droplet size was compared to a sample of droplets an order of magnitude smaller (fig. 3). For the large droplet sample (base area $\sim$ 20 to 3400 μm^2), a small population of droplets crystallizes at small undercooling ($T_c \sim 115\,^{\circ}\mathrm{C}$). These correspond to the most active heterogeneities which are typically responsible for nucleation in the bulk. Upon further cooling, the majority of droplets crystallize between 105 °C and 90 °C. The broad range of temperatures suggests a broad range of heterogeneities within these droplets with widely differing nucleating ability, although less active than the first population. Finally, a small population of droplets crystallizes within a narrow range at 84 °C. The range of crystallisation temperatures observed from this study is in agreement with previous work on similarly sized PE droplets [3].

The data for the larger distribution of droplets is in contrast with that of the sample for droplets an order of magnitude smaller (base area $\sim$ 5 to 350 μm^2). For this case, greater undercooling is required before the onset of crystallisation occurs at 108 °C, with relatively few crystallisation events until the temperature falls below 100 °C. There still exists an intermediate population of nucleation in the range of 87 °C to 100 °C. However, this population is now significantly smaller, representing only 40% of the total crystallised population, compared to almost 80% for the larger droplet sample. Instead, the majority of droplets crystallize at $\sim$ 84 °C (60% of the crystallised population nucleate at this lowest temperature compared to 20% for the large droplet sample). Given the sample preparation method, these results should not be surprising. Assuming a roughly fixed number of heterogeneities in the initial PE film, the chance for defect-free nucleation increases as the droplets are made smaller, simply because this produces significantly more droplets on a sample. The smaller droplet size is consistent with the need to cool to lower temperatures before the onset of crystallisation, and the much larger population nucleating at 84 °C.

3.2 Correlation analysis of crystallization upon cooling

Since heterogeneous nucleation reduces the activation barrier, homogeneous nucleation is the result of the largest activation energy for forming a crystal nucleus. Thus, larger supercooling is required to initiate the formation of a homogeneous nucleus in comparison with a heterogeneous nucleus. It is tempting to assume that the droplets that crystallised at 84 °C do so via a homogeneous mechanism because this is the lowest crystallisation temperature measured. However, as pointed out previously [8,16, 17,23], it can be difficult to rule out the possibility that weakly active heterogeneities are responsible for the lowest nucleation temperature measured when interpreting fractionated crystallisation data. More rigorous evidence than simply the degree of supercooling is required to make the distinction. We have demonstrated the use of correlation plots as an effective method for differentiating homogeneous from heterogeneous crystallisation in a system of dewetted PEO droplets [16]. In a correlation plot, the temperature that a droplet nucleates at in a cooling experiment is plotted as a function of the temperature at which that droplet nucleates in an identical subsequent experiment. Heterogeneous and homogeneous nucleation mechanisms have distinct characteristics that can be differentiated in such a plot. A heterogeneous defect has a fixed

nucleating ability given by its activation energy. A droplet containing a heterogeneity is likely to nucleate at the same temperature in subsequent cooling runs. Furthermore, in a sample with many droplets, there are likely numerous heterogeneities present with varying nucleating ability. As a result, droplets which have nucleated via a heterogeneous mechanism will be strongly correlated and randomly scattered along a line with a slope of one over a relatively large range of temperatures on a correlation plot. In contrast, homogeneous nucleation is a random process intrinsic to the system being studied. Two equally sized droplets have the same probability for creating a crystal nucleus at a given temperature. A distribution of droplets crystallised homogeneously appears symmetrically grouped about the temperature where the nucleation rate peaks, in contrast to the data scattered along the line with a slope of one for the heterogeneous population.

Correlation plots for the two droplet samples discussed above are shown in fig. 4. For the larger droplet distribution (fig. 4a)), the droplets which nucleate in the range of 90 °C to 115 °C are highly correlated and scattered along the line of 1, as expected for a heterogeneous mechanism. While the droplets centred around 84 °C appear to have the symmetric nature characteristic of homogeneous nucleation. In fig. 4a), this population is relatively small and thus difficult to characterize. However, for the sample of smaller droplets shown in fig. 4b), the homogeneous mechanism dominates. The total number of higher-temperature nucleation events is about the same for both samples, which is consistent with the fact that there should be a fixed and similar number of heterogeneities in both initial films. The higher-temperature nucleation events in the smaller droplet sample also possess the characteristics of a heterogeneous mechanism. However, the region of the plot centred around 84 °C is *significantly* more highly populated in the small droplet sample. The symmetric, sharply peaked distribution characteristic of a random, homogeneous mechanism is now clearly evident. As discussed above and shown schematically in fig. 1, when subdividing the sample into more smaller domains it should not be surprising that this region of the plot becomes significantly more populated, supporting the fact that we are observing defect-free nucleation. We conclude that the droplets crystallised between 90 °C and 120 °C in both samples represent heterogeneities of varying nucleating ability, while the droplets centred about 84 °C are nucleated homogeneously. The remainder of this work will focus entirely on the low-temperature homogeneously nucleated population of droplets.

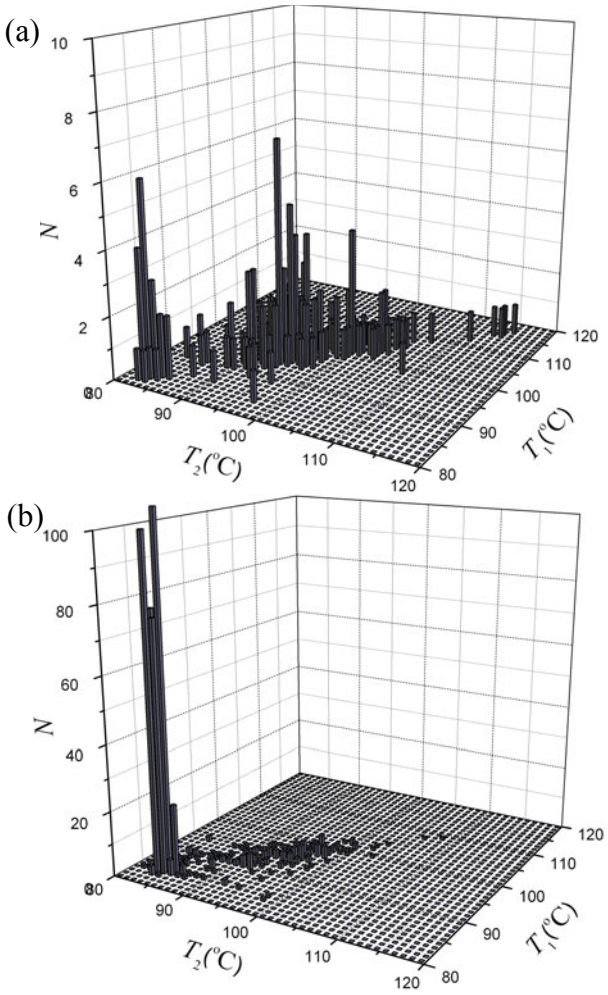

Fig. 4. Correlation plots of the two samples shown in fig. 3 with differing droplet size distributions: a) base area $\sim$ 20 to 3400 μm^2, and b) base area $\sim$ 5 to 350 μm^2. The number of crystallization events in two subsequent cooling experiments for the two samples indicates that the large heterogeneous population peaked at around 95 °C in a) shifts to the low-temperature homogeneous mechanism at 84 °C when the droplets are smaller, b).

3.3 Isothermal crystallization

The second aim of this work is to establish the scaling dependence of the homogeneous nucleation probability upon the size of the PE droplets. Isothermal experiments were performed by quenching the sample rapidly from the melt to 84 °C, the temperature that the homogeneous nucleation rate peaks at in the correlation plots. Assuming an ensemble of equally sized droplets, the rate of change in the amorphous fraction can be written as [17]

$$\frac{\mathrm{d}}{\mathrm{d}t}\left(\frac{N_a}{N}\right) = -P\left(\frac{N_a}{N}\right) = -\frac{1}{\tau}\left(\frac{N_a}{N}\right), \qquad (1)$$

where N_a is the number of amorphous droplets, P is the probability per unit time of having a nucleation event, and τ is the time constant associated with a nucleation event. Thus, we can write $N_a/N = \exp(-t/\tau)$. A plot of the logarithm of the amorphous fraction of droplets as a function of time can be seen in fig. 5. The droplets were binned according to the base area to ensure that droplets of equal volume are being compared (recall that all droplets are self-similar, and $A^{3/2} \propto$ volume). Bin ranges were chosen such that an approximately equal number of droplets populated each range. As an exception, the largest bin size (58 μm^2) was less populated as the dewetting process

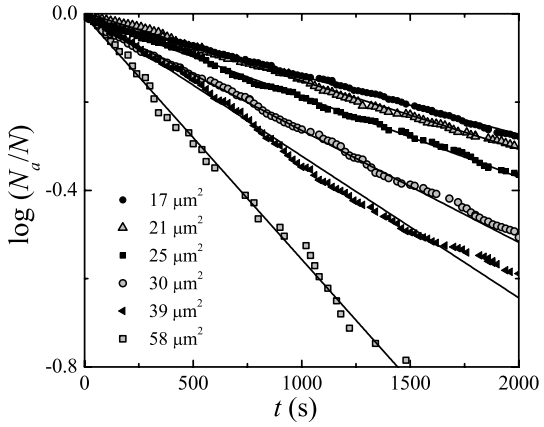

Fig. 5. Logarithm of the amorphous fraction of droplets as a function of time for isothermal crystallisation at $T_c = 84\,^{\circ}$C. The droplets are binned according to their base area as measured by optical microscopy. The centre of the bin range is indicated in the legend. The slope for each data set is related to the time constant, τ, as given in eq. (1), for that particular bin size.

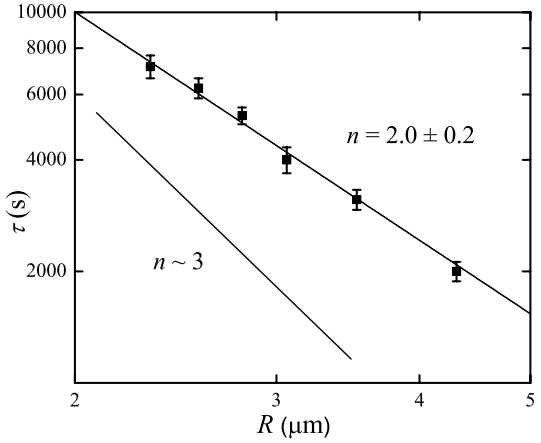

Fig. 6. The scaling of the time constant, τ, as a function of radius, R, of the average droplet base area as measured by optical microscopy for each binned data set. Assuming a relationship $\tau \sim R^{-n}$, a value of $n = 2.0 \pm 0.2$ is measured. This indicates that PE droplets nucleate preferentially at the droplet surface.

resulted in significantly less droplets of the largest size. As expected, the data in fig. 5 is linear for each bin of droplet sizes, in agreement with eq. (1). Furthermore, we observe the expected trend for a random homogeneous nucleation mechanism: the larger a droplet the smaller the time constant for nucleation. In order to quantify how the time constant varies with the size of the droplet, we note that the slope of the best fit straight line for each set of binned data is $-1/\tau$. We write the length scale dependence of the time constant as $\tau \sim R^{-n}$, where R is the average radius of the droplet base area as measured by optical microscopy for a particular bin of droplets. We have previously demonstrated that for a system of PEO droplets on PS, $n \sim 3$, suggesting that nucleation takes place within the bulk volume of a PEO droplet [17,19]. For the PE droplet system, the scaling of τ with droplet length scale, R, is shown in fig. 6. Surprisingly we find that $n = 2.0 \pm 0.2$, and for PE on a PS substrate the nucleation rate is surface dependent. To the best of our knowledge, this is the first direct measurement of the scaling dependence of the nucleation rate for PE micro-domains on the size of the domains.

The fact that the nucleation rate for these droplets of PE is surface dependent may explain some of the observed behaviour noted in the literature regarding PE. A strong dependence between domain volume and crystallisation temperature has been clearly demonstrated in PEO, where exceptionally large supercooling is required as domain size is made much smaller [17,19,24,25]. This observation should be expected for a system where volume-dependent nucleation within the micro-domain has been found. On the other hand, a weaker temperature dependence on length scale has been observed for PE domains [23], consistent with nucleation scaling with the surface area rather than volume. Similarly, different researchers have reported different crystallisation temperatures for PE domains of approximately the same size but different confining matrices. Cases have even been reported where larger PE domains produce lower crystallisation temperatures than smaller domains in other work [23]. These observations may be understood in light of our results. A surface-driven homogeneous nucleation mechanism will be more sensitive to differences in interfacial energy than a volume-dependent mechanism, and thus more likely to be affected by different confining environments. We have recently demonstrated volume, surface and line nucleation in a system of PEO droplets through the use of a tuneable substrate [21]. A large difference in supercooling was measured between the three different nucleation mechanisms with volume-dependent nucleation requiring significantly larger supercooling. In fig. 4, the difference in supercooling between heterogeneous and homogeneous nucleation for PE domains is relatively small compared to PEO droplets. In the case of similarly sized PEO droplets the difference between homogeneous and heterogeneous nucleation was found to be greater than 40 °C [16]. From our analysis, we cannot determine whether the nucleus is forming preferentially at the PE/PS interface, the PE/air interface, or non-preferentially at both. However, what is clear is that for systems of PE domains, nucleation occurs at the interface and the interfacial energy plays a large role in how chains align to form a crystal nucleus.

4 Conclusions

We have utilized a system of dewetted droplets to study crystal nucleation in PE. This technique is unique in its ability to follow crystal nucleation in real time, droplet by droplet, while allowing a direct correlation of these results with the size of individual droplets. We have been able to differentiate populations of droplets nucleating

by heterogeneous and homogeneous mechanisms. A detailed lengthscale analysis of the homogeneous population of droplets reveals that the nucleation is a surface-driven mechanism for droplets of PE on a PS substrate. Simply put, a PE droplet with twice the surface area has twice the homogeneous nucleation probability. The dependence on surface area is consistent with the great variability found in the literature for the temperature at which micro-domains of PE nucleate in different confining media.

The authors thank Prof. Buckley Crist for valuable discussions and for donating the linear PE, as well as Dr. Michael Massa for valuable discussions. Financial support from NSERC of Canada is gratefully acknowledged.

References

1. B. Vonnegut, J. Colloid Sci. **3**, 563 (1948).
2. D. Turnbull, J. Chem. Phys. **20**, 411 (1952).
3. R. Cormia, F. Price, D. Turnbull, J. Chem. Phys. **37**, 1333 (1962).
4. J. Koutsky, A. Walton, E. Baer, J. Appl. Phys. **38**, 1832 (1967).
5. H. Frensch, P. Harnischfeger, B. Jungnickel, Interface **4**, 20 (1989).
6. M. Arnal, M. Matos, R. Morales, O. Santana, A. Müller, Macromol. Chem. Phys. **199**, 2275 (1998).
7. R. Tol, V. Mathot, G. Groeninckx, Polymer **46**, 383 (2005).
8. P. Barham, D. Jarvis, A. Keller, J. Polym. Sci. Polym. Phys. Ed. **20**, 1733 (1982).
9. Y.L. Loo, R.A. Register, A.J. Ryan, Phys. Rev. Lett. **84**, 4120 (2000).
10. G. Reiter, G. Castelein, J.U. Sommer, A. Röttele, T. Thurn-Albrecht, Phys. Rev. Lett. **87**, 226101 (2001).
11. A. Lorenzo, M. Arnal, A. Müller, A. Boschetti de Fierro, V. Abetz, Eur. Polym. J. **42**, 516 (2006).
12. J. Carvalho, M. Massa, K. Dalnoki-Veress, J. Polym. Sci., Part B: Polym. Phys. **44**, 3448 (2006).
13. S. Nojima, Y. Ohguma, S. Namiki, T. Ishizone, K. Yamaguchi, Macromolecules **41**, 1915 (2008).
14. T. Cai, Y. Qian, Y. Ma, Y. Ren, W. Hu, Macromolecules **42**, 3381 (2009).
15. E. Woo, J. Huh, Y. Jeong, K. Shin, Phys. Rev. Lett. **98**, 136103 (2007).
16. M. Massa, J. Carvalho, K. Dalnoki-Veress, Eur. Phys. J. E **12**, 111 (2003).
17. M. Massa, K. Dalnoki-Veress, Phys. Rev. Lett. **92**, 255509 (2004).
18. M. Massa, M. Lee, K. Dalnoki-Veress, J. Polym. Sci., Part B: Polym. Phys. **43**, 3438 (2005).
19. M. Massa, J. Carvalho, K. Dalnoki-Veress, Phys. Rev. Lett. **97**, 247802 (2006).
20. W. Hu, T. Cai, Y. Ma, J. Hobbs, O. Farrance, G. Reiter, Faraday Discuss. **143**, 129 (2009).
21. J. Carvalho, K. Dalnoki-Veress, Phys. Rev. Lett. **105**, 237801 (2010).
22. Z. Wang, B. Hsiao, E. Sirota, S. Srinivas, Polymer **41**, 8825 (2000).
23. A. Müller, V. Balsamo, M. Arnal, *Block Copolymers II, Springer Adv. Polym. Sci.*, Vol. **190** (Springer, 2005) pp. 1–63.
24. H. Chen, S. Hsiao, T. Lin, K. Yamauchi, H. Hasegawa, T. Hashimotos, Macromolecules **34**, 671 (2001).
25. A. Röttele, T. Thurn-Albrecht, J. Sommer, G. Reiter, Macromolecules **36**, 1257 (2003).